Electronic Supplementary Material (ESI) for Journal of Materials Chemistry A.
This journal is © The Royal Society of Chemistry 2023

Electronic supplementary information

A biodegradable, highly sensitive and multifunctional mechanical sensor based on rGO-silk fibroin hydrogel for human motion detection and gesture recognition

Ke Chen,[a] Baoyang Liu,[a] Ning Hu,[a] Qiaolin Fan,[a] Fawang Zhan,[b] Zhou Zhang,[b] Zhonghua Ni,[a] Xiao Li,[a] Tao Hu[a]**

[a] School of Mechanical Engineering, and Jiangsu Key Laboratory for Design and Manufacture of Micro-Nano Biomedical Instruments, Southeast University, Nanjing 211189, Jiangsu Province, China

[b] Central South (Shangrao) Metallurgical Industry Research Institute Co., Ltd. Shangrao, 334000, Jiangxi Province, China

Corresponding Author

*E-mail: hutao@seu.edu.cn (Tao Hu), lx2016@seu.edu.cn (Xiao Li)

This file contains:

S1. Supporting figures: Figure S1~S18

S2. Supporting tables: Table S1~S5

S3. Supporting video for human-machine interaction

S1. Supporting figures: Figure S1~S17

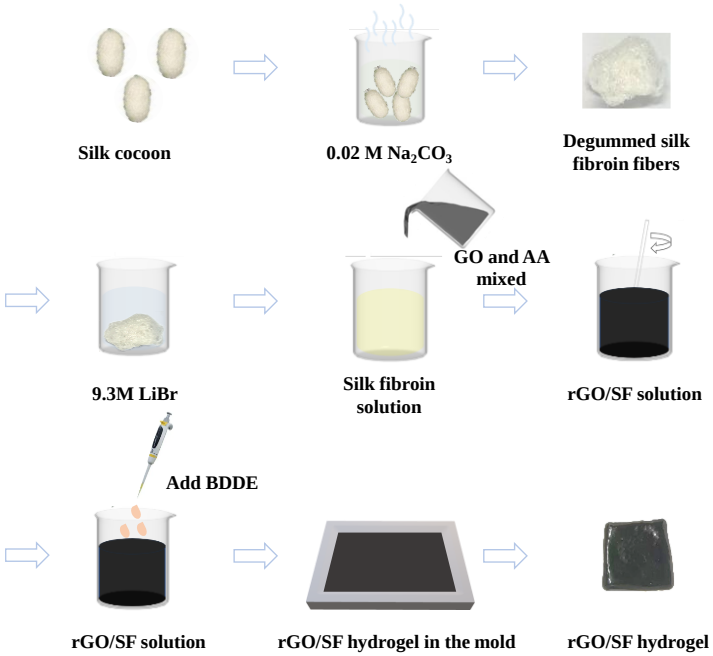

Figure S1. Fabrication process of rGO/SF hydrogel

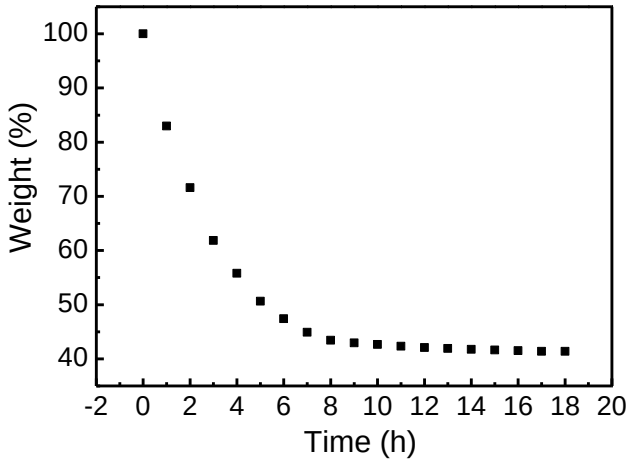

Figure S2. Mass change of rGO/SF hydrogel in room temperature condition

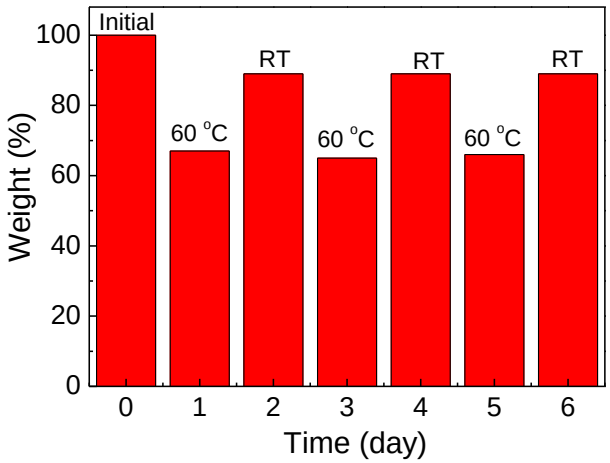

Figure S3. The moisturizing property of rGO/SF hydrogel

Figure S4. Picture of the criterion electromechanical test equipment

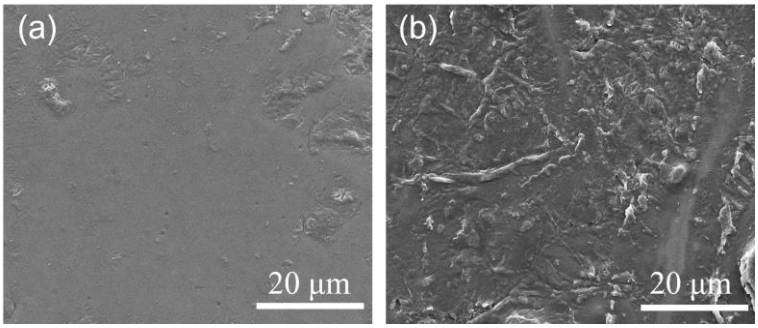

Figure S5. SEM images of the surface morphology of (a) pure silk fibroin hydrogel; (b) rGO/SF hydrogel

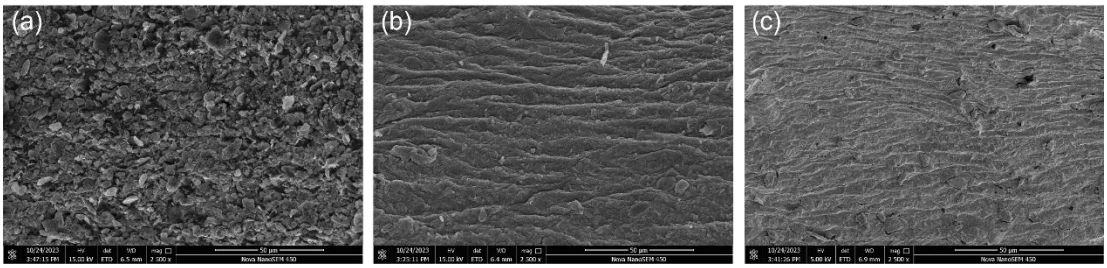

Figure S6. SEM images of the internal structure of rGO/SF hydrogel (a) at its original state, (b) after strain sensing, (c) after pressure detection.

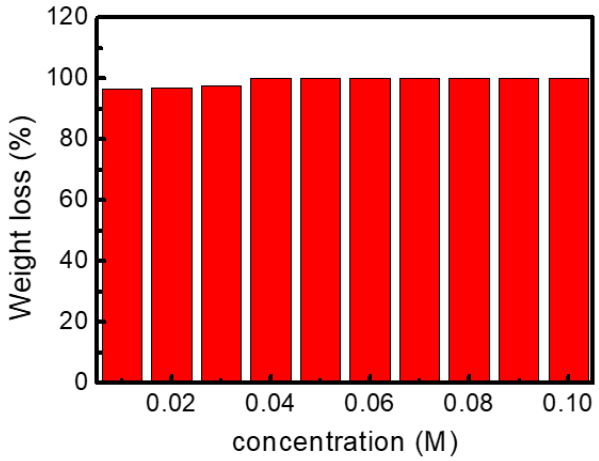

Figure S7. Degradation effect of NaOH solution with different concentration.

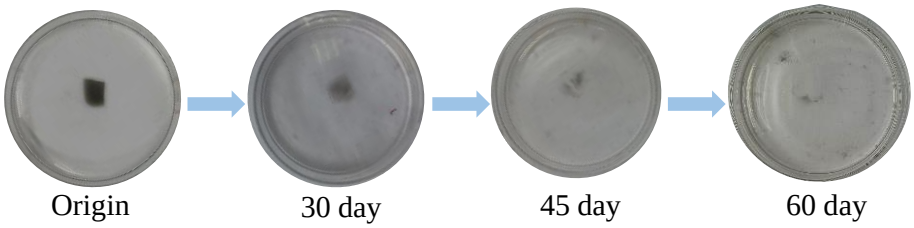

Figure S8. Degradation assessment of rGO/SF hydrogel. Sequential photographs of degradation of rGO/SF hydrogel placed in deionized water.

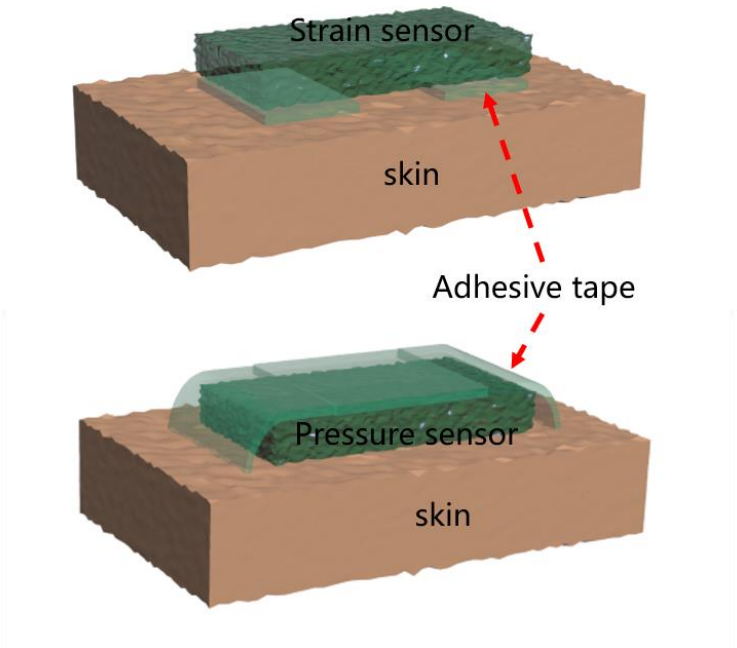

Figure S9. Schematic diagram of tension test and pressure test for human signals detection.

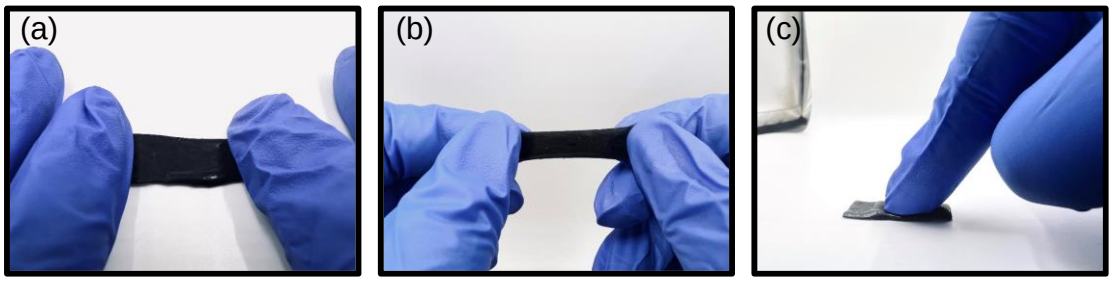

Figure S10. Photographs of rGO/SF hydrogel. (a) original; (b) strain; (c) pressure.

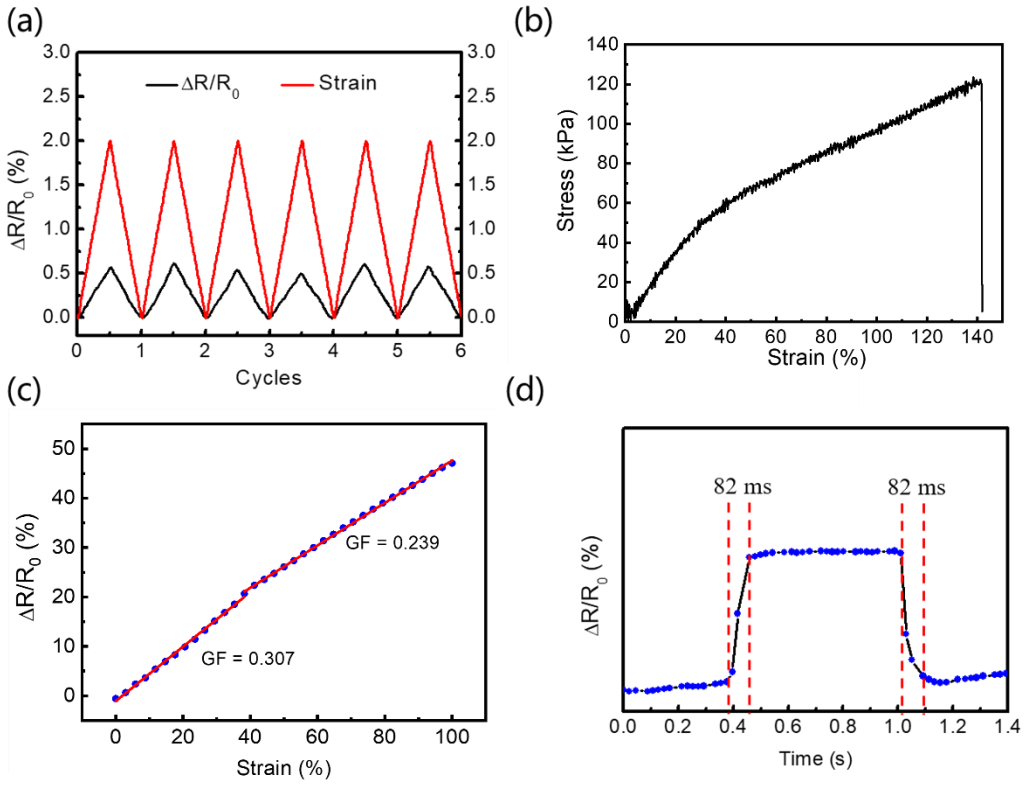

Figure S11. Performance of the rGO/SF strain sensor. (a) Diagram of cycling strain; (b) Diagram of strength limit of rGO/SF strain sensor; (c) Gauge factors of the rGO/SF strain sensor; (d) Response time of rGO/SF strain sensor.

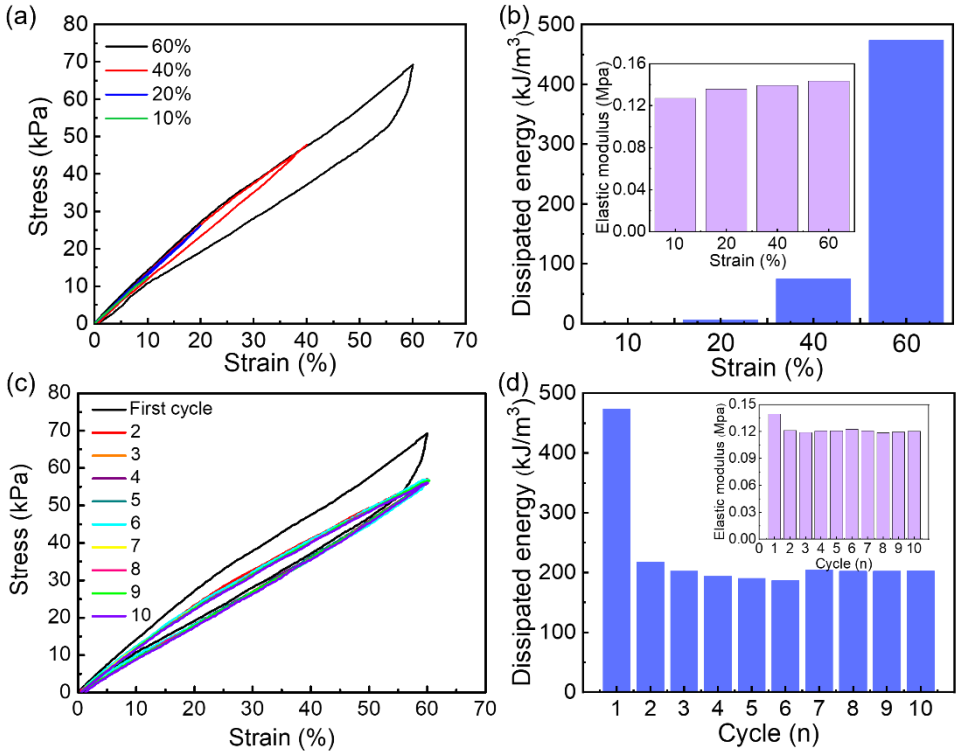

Figure S12. The loading-unloading tests of the rGO/SF hydrogel under various

conditions. (a) Tensile stress-strain curves and (b) corresponding dissipated energy at different maximum strain; (c) Ten successive cyclic stress-strain curves at maximum strain of 60%. (d) The dissipated energy with regard to different cycle. (Insets in (b) and (d) are the corresponding value of elastic modulus)

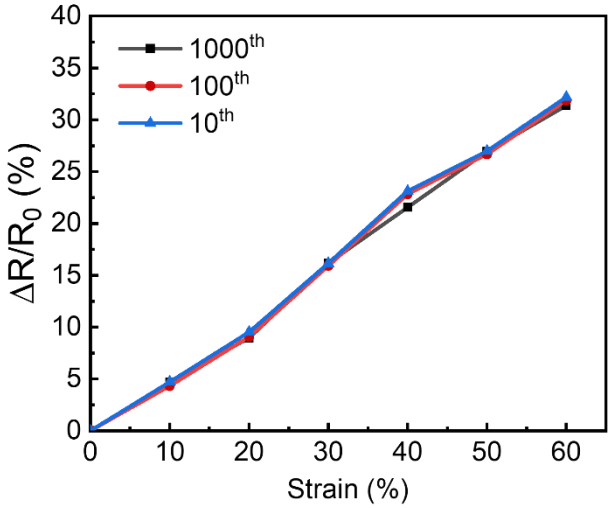

Figure S13. Relative change in resistance versus strain curves for 10 (blue), 100 (red), and 1000 (black) cycles with the strain ranging from 0% to 60%.

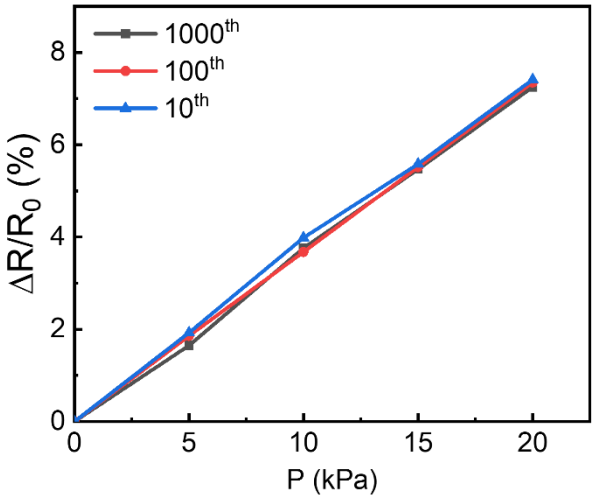

Figure S14. Relative change in resistance versus pressure curves for 10 (blue), 100 (red), and 1000 (black) cycles with the pressure ranging from 0 kPa to 20 kPa.

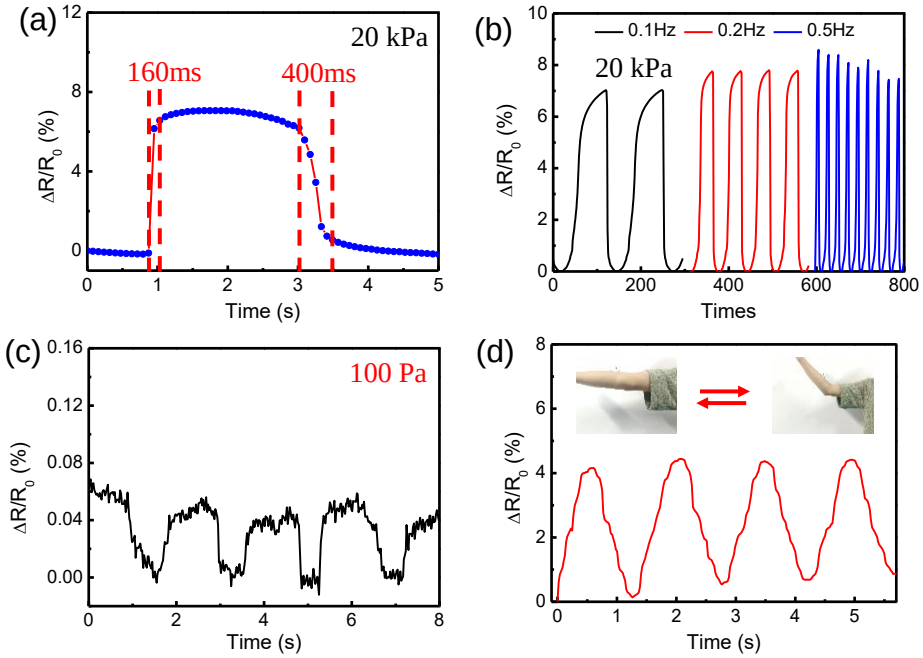

Figure S15. Performance of the rGO/SF pressure sensor. (a) Response time of rGO/SF pressure sensor; (b) Relative resistance variation under cycling stretching/releasing at frequencies of 0.2, 0.5 and 1 Hz; (c) Detection limit test of pressure sensor; (d) Signal responses at elbow joint bending.

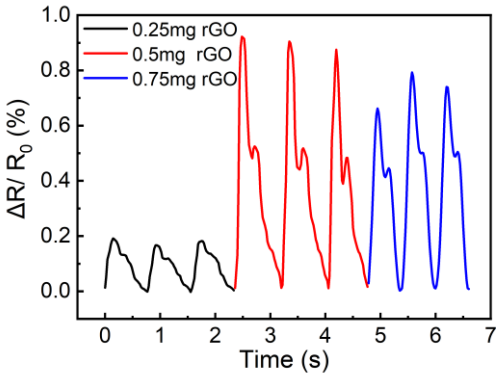

Figure S16. Detection of pulse signals at different concentration of rGO

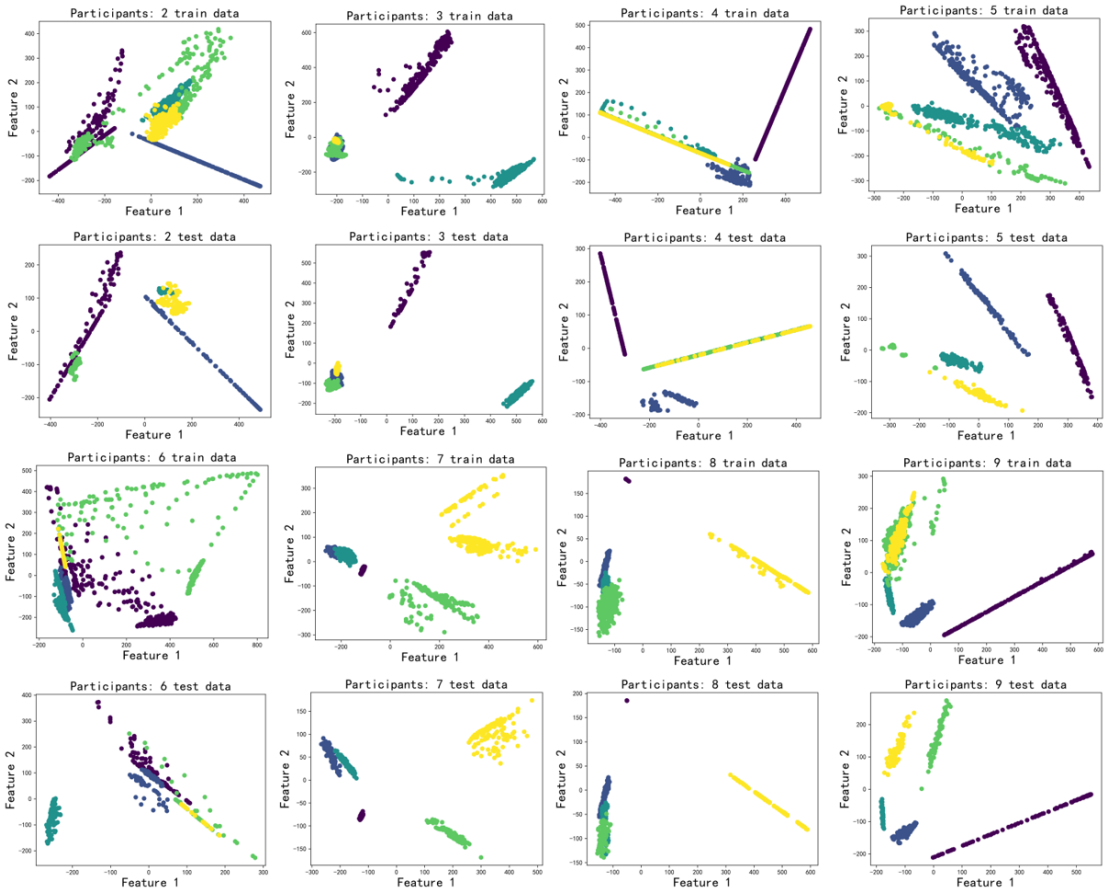

Figure S17. The PCA visualization of the train data and test data of Participant 2-9.

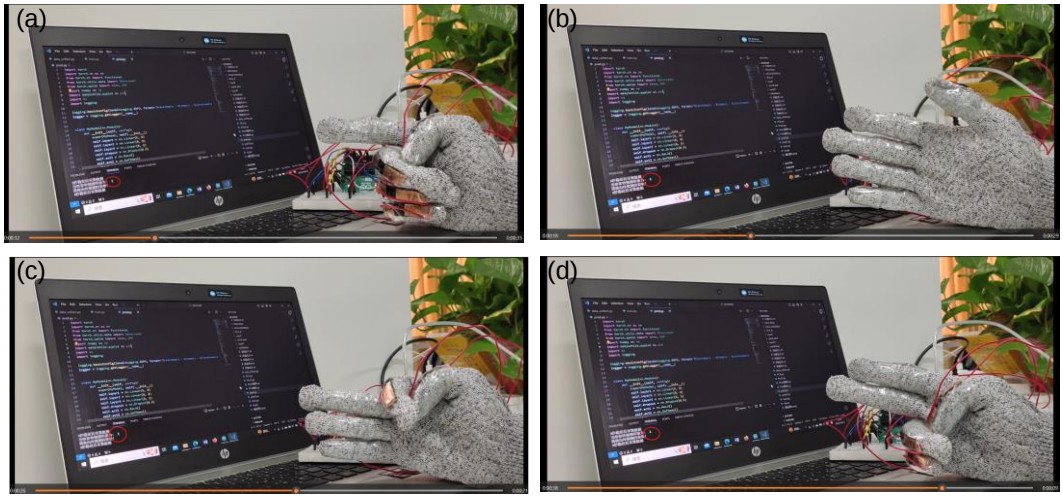

Figure S18. Human-machine recognition of (a) gesture 1; (b) gesture 5; (c) gesture 3; (d) gesture 2.

S2. Supporting tables: Table S1~S5

Table S1. Comparison of our multifunctional mechanical sensor with current reported strain sensors and pressure sensors

Sensing device	Materials	Dynamic range	Sensitivity	References
Strain sensor	CNT/Ecoflex	900%	0.54(0-400%)	S1
Strain sensor	SWCNT/PDMS	280%	0.82(<40%) 0.06(60%-200%)	S2
Pressure sensor	CNT/Ecoflex	700%	0.65(<400%)	S3
Pressure sensor	CNT/Ecoflex	0.1Pa-130kPa	0.601kPa^{-1} (<5kPa) 0.077kPa^{-1} (30-130kPa)	S4
Pressure sensor	rGO/Ag	40kPa	0.016kPa^{-1}	S5
Pressure sensor	rGO/PI		0.18kPa^{-1} (0-1.5kPa) 0.023kPa^{-1} (3.5-6.5kPa)	S6
Pressure and strain sensor	**rGO/SF**	**>500kPa (Pressure) 100% (Strain)**	**Pressure: 0.4kPa^{-1} (0.1-100kPa)、0.1kPa^{-1} (100-500kPa) Strain: 0.307(<41%)、0.239(41-100%)**	**Our sensor**

Table S2. Test accuracy of individual personalized gesture recognition systems

Participants	Accuracy
Participants1	≈95%
Participants2	≈90%
Participants3	≈90%
Participants4	≈90%
Participants5	≈80%
Participants6	≈100%

Participants7	≈100%
Participants8	≈100%
Participants9	≈95%

Table S3. Size of Hidden Layers

Hidden size1	Hidden size1	Accuracy
64	256	≈40%
64	128	≈40%
64	64	≈60%
32	64	≈60%
32	32	≈60%
16	32	≈60%
16	16	≈60%
8	16	≈60%
8	8	≈80%
4	8	≈60%
4	4	≈60%

Table S4. Learning rate

Learning rate	Accuracy
1e-2	≈40%
1e-3	≈80%
1e-4	≈50%
1e-5	≈55%

Table S5. Batch size

Batch size	Accuracy
64	≈50%
32	≈60%
16	≈60%
8	≈80%
4	≈60%

References

S1. Seongwoo Ryu, Phillip Lee, Jeffrey B. Chou, Ruize Xu, Rong Zhao, Anastasios John Hart, Sang-Gook Kim. ACS Nano, 2015, 9, 5929.

S2 Takeo Yamada, Yuhei Hayamizu, Yuki Yamamoto, Yoshiki Yomogida, Ali Izadi-Najafabadi, Don N. Futaba, Kenji Hata. Nature Nanotechnology. 2011, 6, 296.

S3 Park Sun-Jun, Kim Joshua, Chu Michael, Khine Michelle. Advanced Materials Technologies. 2016, 1, 1600053.

S4 Kwon Donguk, Lee Tae-lk, Shim Jongmin, Ryu Seunghwa, Kim Min Seong, Kim Seunghwan, Kim Taek-Soo, Park Inkyu. ACS Applied Materials & Interfaces. 2016, 8, 16922.

S5 Xuchu Dong, Yong Wei, Song Chen, Yong Lin, Lan Liu, Jing Li. Composites Science and Technology. 2018, 155, 108.

S6 Yuyang Qin, Qingyu Peng, Yujie Ding, Zaishan Lin, Chunhui Wang, Ying Li, Jianjun Li, Ye Yuan, Xiaodong He, Yibin Li. ACS Nano, 2022, 9, 8933.

S3. Supporting video for human-machine interaction

(We have uploaded as a supporting video)